

Article

# High-Speed, Helical and Self-Coiled Dielectric Polymer Actuator

Johannes Mersch <sup>1,2,\*</sup> , Markus Koenigsdorff <sup>2</sup> , Andreas Nocke <sup>2</sup>, Chokri Cherif <sup>2</sup> and Gerald Gerlach <sup>1</sup> 

<sup>1</sup> Institute of Solid State Electronics, Technische Universität Dresden, 01062 Dresden, Germany; Gerald.Gerlach@tu-dresden.de

<sup>2</sup> Institute of Textile Machinery and High Performance Material Technology, Technische Universität Dresden, 01062 Dresden, Germany; Markus.Koenigsdorff@tu-dresden.de (M.K.); Andreas.Nocke@tu-dresden.de (A.N.); Chokri.Cherif@tu-dresden.de (C.C.)

\* Correspondence: Johannes.Mersch@tu-dresden.de; Tel.: +49-351-463-33766

**Abstract:** Novel actuator materials are necessary to advance the field of soft robotics. However, since current solutions are limited in terms of strain, strain rate, or robustness, a new actuator type was developed. In its basic configuration, this actuator consisted of four layers and self-coiled into a helix after pre-stretching. The actuator principle was a dielectric polymer actuator. Instead of an elastomer, a thin thermoplastic film, in this case polyethylene, was used as the dielectric and the typically low potential strain was amplified more than 40 times by the helical set-up. In a hot press, the thermoplastic film was joined together with layers of carbon black employed as electrodes and a highly elastic thermoplastic polyurethane film. Once the stack was laser cut into thin strips, they were then stretched over the polyethylene (PE) film's limit of elasticity and released, thus forming a helix. The manufactured prototype showed a maximum strain of 2% while lifting six times its own weight at actuation frequencies of 3 Hz, which is equivalent to a strain rate of 12%/s. This shows the great potential of the newly developed actuator type. Nevertheless, materials, geometry as well as the manufacturing process are still subject to optimization.

**Keywords:** artificial muscle; dielectric polymer actuator; soft actuator; self-coiled actuator; self-sensing



**Citation:** Mersch, J.; Koenigsdorff, M.; Nocke, A.; Cherif, C.; Gerlach, G. High-Speed, Helical and Self-Coiled Dielectric Polymer Actuator. *Actuators* **2021**, *10*, 15. <https://doi.org/10.3390/act10010015>

Received: 11 December 2020

Accepted: 12 January 2021

Published: 15 January 2021

**Publisher's Note:** MDPI stays neutral with regard to jurisdictional claims in published maps and institutional affiliations.



**Copyright:** © 2021 by the authors. Licensee MDPI, Basel, Switzerland. This article is an open access article distributed under the terms and conditions of the Creative Commons Attribution (CC BY) license (<https://creativecommons.org/licenses/by/4.0/>).

## 1. Introduction

Soft robotics is an emerging field with the potential to overcome the limitations of classic, rigid mechanisms [1,2]. An extensively researched field involves soft actuators, often called artificial muscles, giving soft robotic systems the ability to interact with and in combination with integrated sensors react to their environment [3]. Many of the employed principles and demonstrator structures are inspired by biological role models [4–6]. Possible motions are, for example, locomotion, transportation, or gripping [7–9]. The aim to give the soft robotic systems the ability to move and manipulate objects in their environment make it necessary for the structures to incorporate potent actuators and sufficiently precise sensors that allow for proprio- and exteroception. Similar to how muscles and nerves allow animals to perform complex tasks. Frequently employed actuator mechanisms include pneumatics, thermally responding materials like shape memory alloys (SMA) or polymers, or dielectric elastomers actuators (DEA) [10–13]. The former exhibit large potential strain and force but also require additional compressors to supply pressurized air for actuation; the resulting systems are bulky and less portable apart from possessing highly nonlinear dynamic behavior and low efficiency. Actuators stimulated by external heat sources or Joule heating, for example, SMAs, have a high work density and can exert high forces at moderate strain levels [14]. However, they also exhibit strong hysteresis and are very slow especially while cooling [15]. Novel actuator types, such as twisted, coiled polymer actuators, are a promising new option due to their lower hysteresis and lower costs [16,17]. Unfortunately, they still lack efficiency, do not have a powerless halting state and are slow to

relax unless actively cooled. Incorporating these slower active components into minimum energy structures does allow for faster motions of the overall system. Moreover smartly combining several actuators to move out of the resting positions can also circumvent the problem of an energy consuming halting state [18]. Still, this is only feasible for specialized structures with two desired states. As that is not desired for many versatile, flexible, biomimetic systems, these disadvantages persist.

DE actuators, in contrast, provide large strains (>300%), high speeds, self-sensing capabilities, and can be held in their activated state without further power consumption [19]. However, current DEAs require rigid frames to be pre-strained. Otherwise, their strain is reduced by several orders of magnitude [10]. Other challenges in DEA technology are posed by the manufacturing of stable, compliant electrodes, the prevention of a dielectric breakdown, and the expanding nature of DEAs when actuated, which is contrary to natural muscle function [20]. Additionally, the most frequently used materials, for example, acrylic and silicone membranes, are difficult to manufacture and reliably handle at thicknesses below 100  $\mu\text{m}$  [21]. Moreover, these thin elastomer films are prone to mechanical defects and dielectric breakdown. These disadvantages severely limit their potential since the electrostatic pressure

$$P_{\text{eq}} = \varepsilon_0 \varepsilon_r \left( \frac{U^2}{t^2} \right) \quad (1)$$

responsible for actuation can be increased by decreasing the dielectric's thickness  $t$ .

The alternative would be to increase the applied voltage  $U$  or the permittivity  $\varepsilon$ —an option that is limited by breakdown strength, safety concerns, and the availability of compact high-voltage power supplies. The relative permittivity  $\varepsilon_r$ , which ranges from two to five for common dielectrics, can be improved by additives, which in return lower breakdown strength and stretchability [22].

Thus, the feasible Maxwell pressure and electromechanical coupling of pure elastomer membrane actuators are considerably restricted.

Some of these disadvantages are addressed by the hydraulically amplified self-healing electrostatic (HASEL) actuator that combines electrostatic and hydraulic actuation by means of a thin, polypropylene film [23]. In contrast to silicone dielectric membranes that exhibit strains over 300%, strains are negligible because of their relatively high mechanical stiffness  $Y$  ( $\sim 0.1$  MPa for typical elastomers, up to  $\sim 1500$  MPa for polypropylene) if thermoplastic materials, such as polyethylene or polypropylene, are used as dielectric. The achievable strain

$$s_z = \frac{P_{\text{eq}}}{Y}, \quad (2)$$

is approximately 0.25% for a 10  $\mu\text{m}$  film with 1500 MPa at 5 kV.

The HASEL actuator exceeds those limits by moving a dielectric liquid in a sealed pocket of thin thermoplastic films [24]. This actuator can be manufactured from inexpensive materials by industrial processes and demonstrate large forces at high speeds as well as good maximum strains. However, the strain is limited to approximately 20% in addition to a leakage of hydraulic fluids potentially lowering long-term stability and reliability.

Therefore, in this article, a novel type of actuator based on a self-coiling dielectric polymer actuator (DPA) will be introduced. It is inspired by the fiber-based artificial muscles presented by Kanik et al. [25]. Kanik's fibers consist of two polymers that are processed by thermal drawing to cross-sections of 13 by 8  $\mu\text{m}$ . Although the difference in thermal expansion coefficients of  $10^{-4} \text{ K}^{-1}$  is relatively small, when converted to a spring shape by cold drawing, the fibers contract by 50% with a temperature difference of only 14 K. Evidently, an elongation difference of 0.14% in the bi-polymer leads to a global contraction of 50%.

Regardless of their impressive performance, these fibers still exhibit poor dynamic behavior. Upon cooling after activation, the heat introduced during the activation process must be dissipated. If a number of these fibers are combined to a bundle, as is the case in natural muscles, the heat dissipation and consequently cooling rate can be lowered

even further. In contrast, an electroactive actuator is incredibly fast, while its dynamic performance is often limited by the mechanical structure's inertia rather than the actuation principle. Additionally, dielectric elastomer actuators also inherently offer the possibility to self-sense their position [26,27].

Twisted or helical fibers are still a very interesting and promising research approach for actuators [28]. Therefore, in this article a self-coiled dielectric thermoplastic actuator is developed and characterized.

The presented helical, fiber-shaped actuator consists of four layers as illustrated in Figure 1a, i.e., one thermoplastic elastomer of thermoplastic polyurethane (TPU) layer, one thermoplastic in this case polyethylene (PE) layer, and two electrodes made of carbon black (CB) on both sides of the thermoplastic. The active layer of the set-up is the thermoplastic layer, which is compressed when an electric voltage is applied to the electrodes. Due to the high elastic modulus, the resulting strain is low in the case of practical excitation voltages, 0.25% for 5 kV (see Figure 1b). The active PE layer is made from standard plastic wrap. After joining the four layers, the layered set-up is stretched over the PE's elastic limit and deformed plastically. The elastically deformed TPU recovers its original length and upon release below the critical force, the fibers coil into a helix. The critical force as well as the parameters of the resulting helix can also be predicted using analytical models [29]. Higher pre-strain and therefore a larger discrepancy in the relaxed lengths of the layers, leads to a higher number of turns per length and smaller coil diameter.

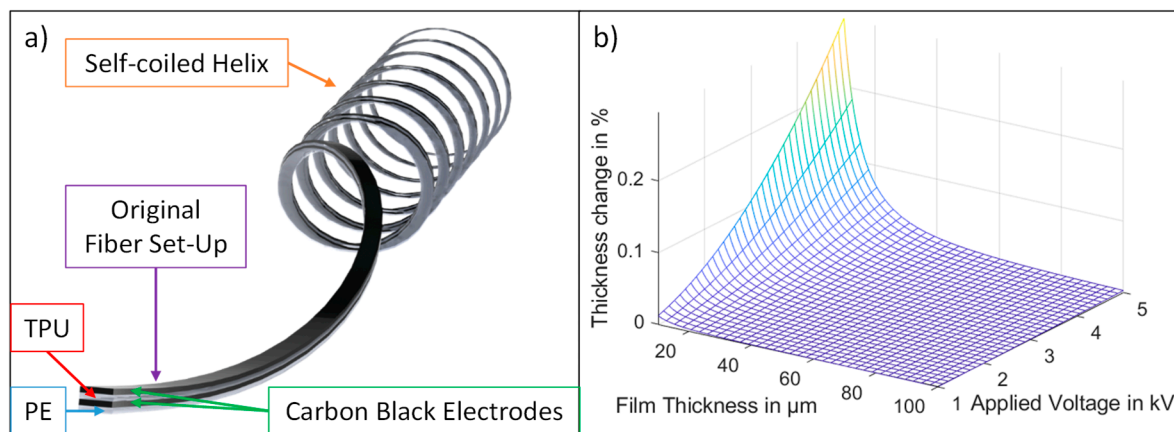


**Figure 1.** (a) Helical fiber actuator set-up; (b) theoretical prediction of the deformation of a dielectric elastomers actuator (DEA) with an elastic modulus of 1500 MPa at varying thicknesses and voltages.

When a high potential difference is applied to the electrodes, the PE layer is compressed and consequently expands equilaterally; as a result, the diameter of the helix increases, while its length decreases. The global contraction of the helix is far larger than that of a straight compressed PE layer would be. The developed actuator type is fiber-shaped, has very low reaction times, can potentially produce strains similar to natural muscle, and has self-sensing capabilities, thus making it a promising new alternative for artificial muscle applications. In the following section, a brief overview over the manufacturing process and resulting actuator specimens will be given. Subsequently, the manufacturing process and the behavior of specimens under actuation as well as their self-sensing performance when loaded externally will be presented.

## 2. Materials and Methods

The base materials used in this study are packaging stretch wrap, CB and a hyperelastic film. As usual for stretch wrap, the film is made of linear low-density polyethylene (LLD-PE), which according to the Omnexus Plastics Database has a dielectric constant and dissipation factor of 2.3 and 0.0003 at 1 kHz, respectively (Stretchfolie 270 m Transparent, purchased at Golder Handels GmbH, Eching, Germany). These films had thicknesses of

12 and 23  $\mu\text{m}$ . For the conductive percolation system, the pure CB powder Ketjenblack EC-600JD (AkzoNobel N.V., Amsterdam, The Netherlands) was used, which is highly suitable for electro-conductive applications due to its morphology and high surface area. As the hyperelastic material, a 100  $\mu\text{m}$  thick TPU film (bonobo repair, Gosen-Neu Zittau, Germany) was selected. Other materials used in the experiments include carbon nano tubes (NC7000, Nanocyl SA, Sambreville, Belgium), conductive epoxy (L100, Kemo Electronic GmbH, Geestland, Germany) and conductive yarn (Shieldex 100 Micron, Statex Produktions+Vertriebs GmbH, Bremen, Germany).

To produce helical dielectric polymer actuators according to Figure 1a, a PE film was coated with a CB/isopropyl alcohol mixture with the isopropyl alcohol evaporating at ambient temperature after 10 min. The conducting ink was made by mixing 0.15 g CB with 8.5 g isopropyl alcohol in an ultrasonic bath for 30 min. This mixture was then brushed onto the LLD-PE film. For the electromechanical characterization, the 12  $\mu\text{m}$  film was used. This layer of CB functioned as the inner electrode. In a hot press (P300 PV, Dr. Collin GmbH, Maitenbeth, Germany), the CB was fixated on the PE film by applying a pressure of 10 bar at 130  $^{\circ}\text{C}$  for 2 min. Subsequently, the joined CB-PE film was stacked onto the TPU film and pressed again at 135  $^{\circ}\text{C}$  and 10 bar for 2 min. Next, a second CB-PE film was pressed onto the existing stack to add a second electrode. The resulting stack is depicted in Figure 2c. Optionally, a third PE film for breakthrough prevention or contacting elements, such as thin copper wires, copper foil, conducting epoxy glue or silver-plated yarns, can be inserted.

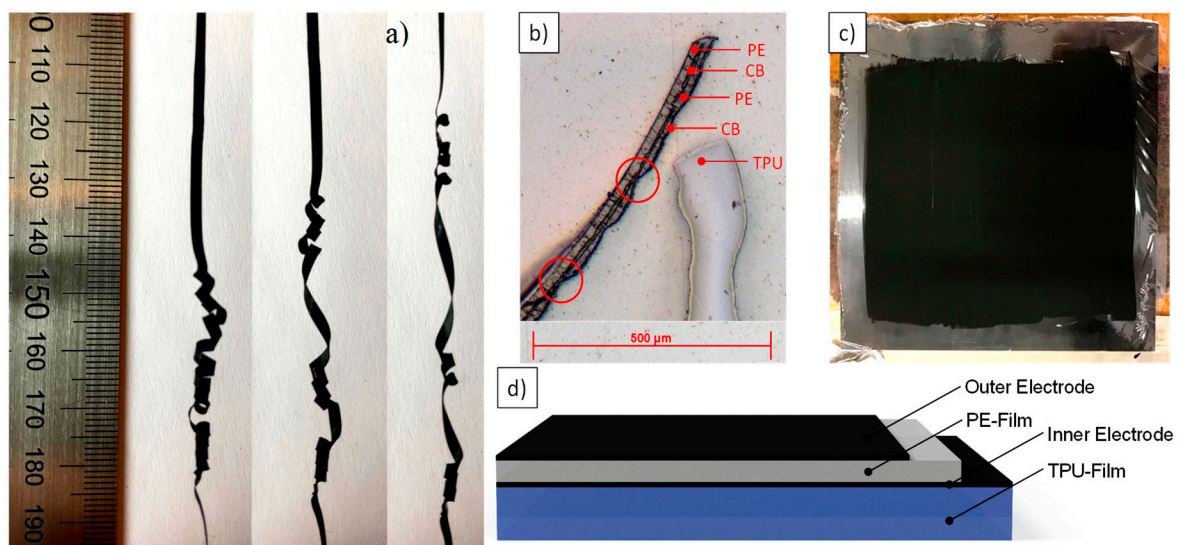


**Figure 2.** Helical dielectric polymer actuator: (a) self-coiled actuator at varying strains; (b) microscopic image of defects occurring during manufacturing: separation of the thermoplastic polyurethane (TPU) layer from the PE layer and thinning of the PE layer resulting in dielectric breakdown; (c) image of the pressed layer stack on the hot press plate before cutting; (d) layer sequence of the functioning helical dielectric polymer actuator.

Afterward, the pressed film stack was cut into thin fibers either manually with a scalpel or by laser cutting. The samples were pre-stretched by 35 to 60% and subsequently released, which led to the formation of several coils over a sample length of approximately 40 mm (Figure 2a). The coiled fibers showed perturbations similar to plant tendrils [30]. Many of the produced samples had one or multiple defects, resulting in the separation of layers, dielectric breakdown or short-circuits (see Figure 2b). These types of defects may occur due to material inhomogeneities, manual handling and electrical contacting. Generally, laser-cut samples are more stable, most likely because fiber edges are sealed during the process, which prevents short-circuits between the inner and outer electrode in case a coil contacts itself. The effect is strongest when the TPU film is located on the upper side of the stack during the laser cutting process. To flatten and prevent the joined stack

from distorting during the laser-cutting process, it is taped on to a sheet of paper that can easily be removed afterward. The laser-cutting was conducted with a Lasermass Plott 60 (Lotus Laser Systems, Basildon, Great Britain, UK) at 70% of the maximum power and a cutting speed of 350 mm/s.

The successfully manufactured specimens were stable up to an activation voltage of 5 kV.

The prepared specimens were tested by attaching small pieces of paper weighing 0.1 g to the end of the coiled actuator. The open source high voltage power source “Peta Pico Voltron” was used for the application of high voltage potential to the electrodes [31]. Since most samples were not stable at potential differences exceeding 5 kV, they were tested at 2 to 5 kV and an excitation frequency of 2 and 3 Hz. The motion was filmed with a digital camera (Lumix, Panasonic, kadoma, Japan) with 30 frames per s, and the images obtained were evaluated with a Matlab (Mathworks Inc, Natick, MA, USA) script using the Eigenvalue features as a position indicator.

The characterization as a sensor was carried out with the pre-stretching device. Varying lengths from 25 to 115 mm were set. At each point, the electrical resistance was measured with a multimeter (DAQ6510-7700, Keithley Instruments, Cleveland, OH, USA).

Microsections were prepared by embedding the fibers in epoxy resin, curing, cutting, and grinding of the cross-section. By means of the microscope Axiolmager (Carl Zeiss AG, Oberkochen, Germany), images of cross-sections were taken and analyzed. Additionally, Differential Scanning Calorimetry of the base materials was conducted to determine the optimal joining temperature.

### 3. Results

#### 3.1. Manufacturing of Helical Dielectric Polymer Actuator

The fabrication process of the fiber-shaped actuator posed several challenges before being able to manufacture working specimens. First, CB was used instead of carbon nano tubes for the electrodes. The carbon nano tubes, even after long dispersion times in planetary centrifugal mixers or in an ultrasonic bath, re-agglomerated quickly after being applied to the PE film. As that problem was significantly reduced with the use of CB, it was chosen as the electrode material. However, a minimal amount of CB particles (0.05%), according to the datasheet, are larger than 45  $\mu\text{m}$  in diameter. That leads to defects in the PE film when these overly large particles are pressed into it.

The Differential Scanning Calorimetry revealed a melting temperature of 122  $^{\circ}\text{C}$  for the used PE film and 158  $^{\circ}\text{C}$  for the TPU film. Because the TPU starts to soften already at 126  $^{\circ}\text{C}$ , the hot press temperature of 135  $^{\circ}\text{C}$  was chosen to join the TPU and PE layers and only 130  $^{\circ}\text{C}$  to join the CB and the PE layer for the outer electrode. In further trial and error tests, this proved to be the optimal temperature values.

Another important factor that leads to poor sample quality is the contacting step. The first approach was to insert additional highly conductive materials on the edges before joining the layers together in order to contact the inner electrode. Inserted aluminum or copper foil lead to very little adhesion between the PE and TPU layers because the stiff metal layers prevented the hot press from fully closing. When using silver-plated polyamide yarn, the adhesion between the layers was significantly better because the press was able to deform the yarn sufficiently. However, during the joining process, the yarn pierced the PE film, which lead to an undesirable electrical connection between the electrodes. Finally, the strategy depicted in Figure 2d was adapted with a slightly reduced length of the PE film, which allows the inner electrode to be contacted easily. For actuation of the samples aluminum or copper foils were folded around the contacting areas for the inner and outer electrode and connected to the high-voltage power source by crocodile clips.

Also the pre-stretching factor is an essential parameter to be considered. As shown in Figure 3a, the TPU base material is stretchable to over 800%. If joined in the hot press with the PE film, the force needed to elongate it, i.e., the modulus, is higher. In the performed

tensile tests, the TPU/PE composite was stable at least up to 150% strain. Above that, the PE layer broke and separated from the TPU layer. As highlighted in Figure 3a, at that point, the strain–stress curve drops to that of the pure TPU film.

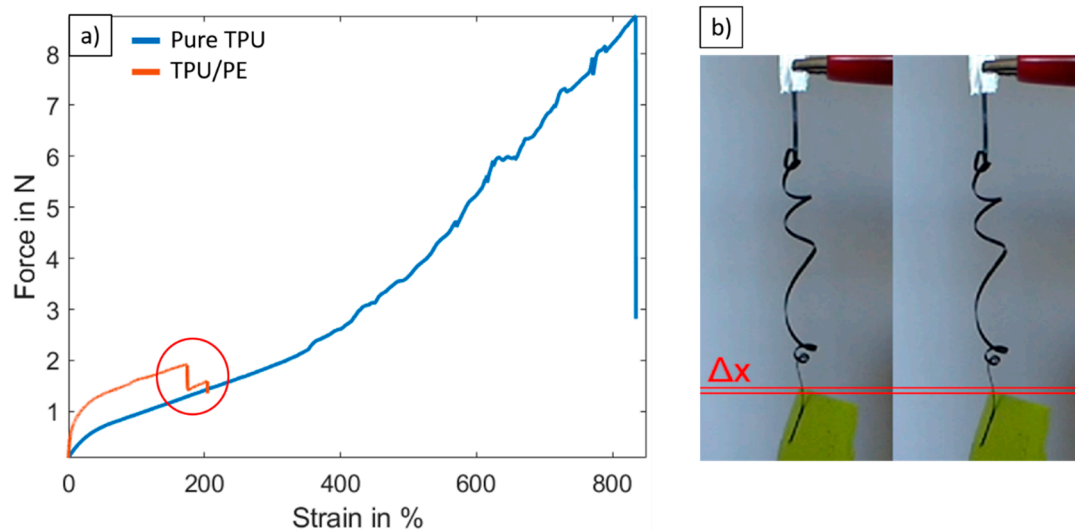


**Figure 3.** (a): Tensile tests of the TPU material and the TPU/PE/CB Composite; (b) helical dielectric polymer actuator (DPA) in activated and inactivated state for an activation potential of 3 kV with  $\Delta x = 0.4$  mm.

Thus, theoretically a pre-strain of 100 or 150% should be feasible. As demonstrated in a previous study, an increase in pre-strain leads to a decrease in spring diameter, which in turn increases contraction upon activation [25]. Therefore, a high amount of pre-strain is desirable to maximize the contraction potential. However, the application of excessive pre-strain leads to damages of the PE film and consequently breakthroughs between the electrodes. Because all samples with an applied pre-strain of more than 60% were defective, the maximum feasible pre-strain was 60%. The characterization was performed with samples with 40% pre-strain to enhance the share of working specimens. The pre-strain of 40% leads to a relatively low number of coils per length, and thus, lower maximum contraction. As visible in Figure 3b the number of turns per cm is approximately two.

To prevent defective samples from being evaluated with high-voltage activation, resistance measurements between the inner and outer electrode were conducted before and after pre-stretching. Only if the resistance exceeded the range of the laboratory multimeter, the samples were evaluated further.

### 3.2. High-Voltage Actuation

When a high-voltage potential is applied to the inner and outer electrodes of the self-coiled actuator, the actuator contracts as expected. Simultaneously the coil diameter increases. Due to the small overall actuator length, the contraction is hardly visible but can be tracked with sufficient accuracy by a high-resolution camera. Without the small weights slightly elongating the fiber, the motion is not directed longitudinally but is random. Therefore the analysis was conducted with these weights.

If there is a small defect in the thermoplastic film that leads to a short circuit, the current flowing through that miniature hole leads to a temperature increase. Subsequently, the film melts at that location and the sample is a defect. The approach to check for these defects beforehand by measuring the resistance between both electrodes was not successful. Most likely because the microscopic damages in the dielectric layer are very small, which together with the high resistance of the electrodes leads to a resistance that exceeded 100 M $\Omega$  and could not be measured with the employed equipment.

Figure 4a shows the results for actuators at varying applied voltages and activation frequencies.

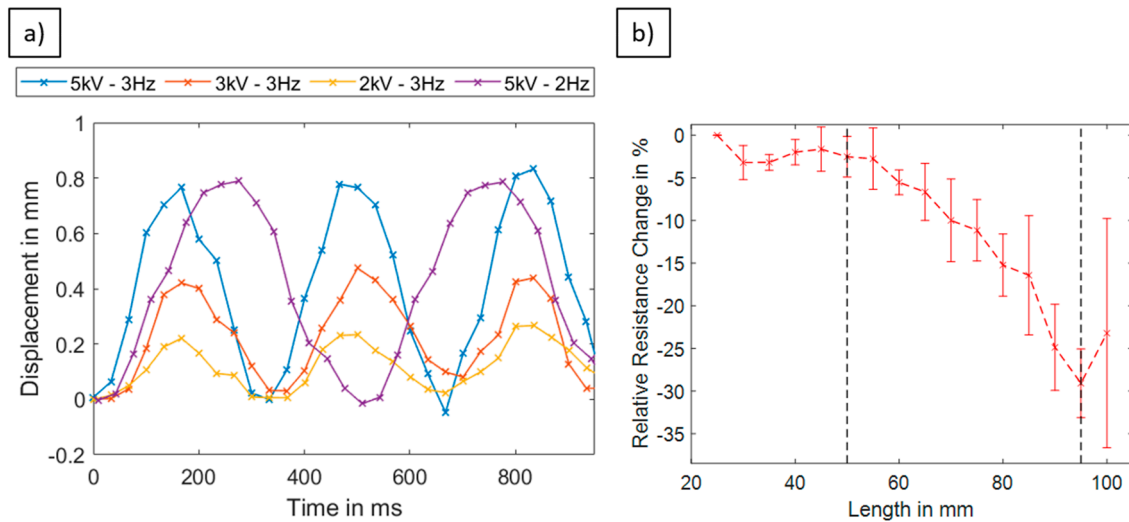


**Figure 4.** Actuation of helical DPA at (a) different activation voltages and frequencies; (b) resistance response of the helical DPA when strained.

When actuated with 5 kV, the samples exhibited a maximum contraction of 0.8 mm, which is equivalent to 2% contraction for the sample of 40 mm length. As expected according to Equation (1), the maximum contraction was lower for 2 and 3 kV with 0.21 and 0.44 mm or 0.52 and 1.1%, respectively. For 3 kV, that contraction was more than 40 times higher than the theoretical thickness change of the PE film (0.025%).

At both excitation frequencies of 2 and 3 Hz, the movement of the attached weight follows the excitation signal well. With a maximum velocity of 4.8 mm/s or a strain rate of 12%/s for both activation and deactivation, the helical DPA offered high-speed actuation. There was no significant difference in maximum contractions between the samples activated at frequencies of 2 and 3 Hz.

### 3.3. Strain Sensing

The developed actuator type offers the potential for self-sensing its position. To evaluate this hypothesis, the resistance of the outer electrode was tracked while passively deforming the helical actuator (Figure 4b). In the overcontracted state, i.e., the coils were in contact with one another, the resistance was stable (under 50 mm length). However, once the specimens were stretched to separate the coils, their resistance decreased until the actuator was fully stretched and all coils disappeared (over 100 mm). In this state, the linearized average resistance change was 25 k $\Omega$ /mm, equaling a gauge factor of  $-1.14$ . When the actuator was stretched even further, thus drastically deforming the electrodes, the electrode resistance abruptly rose again. This behavior was repeatable for several specimens and at least three cycles. After every cycle and the involved overstretching, the base resistance increased. For the second and third cycle, the resistance continued to decrease up to a length of 100 mm in some cases due to the not recovered amount of strain of the first cycle. However, if being stretched to 115 mm, which was only done after the third cycle, the resistance on average rose drastically to 40% of the base resistance. Overall, electrode resistance remained relatively high at 3 M $\Omega$ , which might lead to a transmission line effect for longer fibers.

The negative gauge factor is uncommon for sensors with a percolative system based on a CB or CNT composite. Usually, the resistance increases upon elongation. However, the negative gauge factor is still sensible when considering the self-coiled helical set-up. When activated the dielectric thermoplastic layer expands, which leads to an expansion of the coil diameter and a contraction in fiber direction. Therefore, when elongated by an external force, as in this case, the electrode is compressed rather than stretched leading to a

decreasing resistance. After the helix is stretched so far that it is uncoiled, the electrode is then strained as well, which explains the sharp increase in resistance after this point.

#### 4. Discussion

The newly developed DPA is able to lift at least six times its own weight at rates that are only achievable for thermal actuators if cooled actively. Also, the limit of the weight to be lifted as well as the relation between applied weight and contraction is to be investigated further. The actuator stroke is limited, due to the relatively low number of seven or eight coils over a length of 40 mm.

Another important aspect that must be further investigated and requires optimization is the geometry of individual layers: the thickness ratio of passive and active layers as well as the aspect ratio of the total cross-section are essential factors. If the cross-section is significantly wider than it is high, the actuator not only curls into a helix along its length but in the lateral direction as well, c.f. Figure 2b (microsection). Due to different underlying actuation mechanisms compared to the thermally drawn and actuated fibers by Kanik et al., the optimal cross-section may not necessarily be squared with equal heights of both materials as they suggested for their fiber.

In comparison with the bi-polymer fibers presented by Kanik, the helical dielectric thermoplastic polymer actuators show lower maximum contraction. That is likely due to the significantly lower pre-strain and the following turns per cm (<2 versus a maximum of 16) of the helix. Simultaneously, they can be actuated above frequencies of 1 Hz without water cooling and are significantly less dependent on the ambient temperature. Additionally, in contrast to regular DEAs, they are mechanically robust and do not require a pre-stretching frame during operation.

Moreover, the self-sensing can also be improved. First, better conductivity of the electrodes would facilitate the measurement. Secondly, using a capacitance-based measurement instead of resistance might be beneficial. Especially for dynamic movements, percolative sensor systems based on carbon particles are disadvantageous due to their non-monotonic sensor behavior [32]. Capacitance as a position indicator could provide a monotonic, more linear signal but the strategy to use three electrodes with the aim to minimize the influence of close disturbing objects like the human body would require considerable changes to the actuator concept.

#### 5. Conclusions

A novel sensor-actuator concept for a helical artificial muscle as well as a corresponding prototype structure were successfully developed. In summary, the following conclusions can be given:

1. It is feasible to manufacture a functioning helical dielectric thermoplastic polymer actuator.
2. The actuator can lift multiples of its own weight at actuation frequencies over 1 Hz.
3. Actuator strain is still limited but by far exceeds that of a comparable planar configuration.
4. The helical DPA has the potential to combine the advantages of coiled thermally activated artificial muscles and DEAs.
5. The actuator is capable of self-sensing position control.
6. Actuator materials, geometry, and manufacturing methods are still subject to optimization to significantly improve actuator performance.

The new actuator concept is very promising for applications in soft robotic systems, although still requiring essential modifications. Especially the implementation of stable electrodes and miniaturization of the actuator are promising options for enhanced performance. Additionally, this study was restricted to a single material combination. Materials and manufacturing methods that allow more pre-stretch or enable the production of thinner strips can help to significantly increase contraction. Also, thinner films, both for the PE as well as the TPU layer, could improve the stroke and overall electromechanical coupling. This feature could be realized by the thermal drawing of a four-layer fiber set-up. The vast variety of thermoplastic polymers leaves considerable room for improvement,

and potentially bi-sensitive actuators with suitable material combinations that respond to electrical and thermal stimuli are promising options as well. Moreover, the drastically different elastic moduli of active, inactive, and electrode materials including their relation also influence the actuator performance. Other conducting particles, like carbon nano tubes, might improve electrode conductivity, thus minimizing the transmission line effect or allowing thinner electrode layers.

**Author Contributions:** J.M. developed the actuator concept, designed the experiments, analyzed the data and wrote the paper. M.K. performed and evaluated the experiments. A.N., C.C. and G.G. provided scientific guidance, proof-reading, funding acquisition and laboratory equipment. All authors have read and agreed to the published version of the manuscript.

**Funding:** This research is funded by the DFG research project 380321452/GRK2430, which is supported by the Deutsche Forschungsgemeinschaft (DFG, German Research Foundation). The financial support is gratefully acknowledged.

**Institutional Review Board Statement:** Not applicable.

**Informed Consent Statement:** Not applicable.

**Data Availability Statement:** Data available in a publicly accessible repository. The data presented in this study are openly available in FigShare at 10.6084/m9.figshare.13574036.

**Acknowledgments:** We thank Konrad Katzer (Fraunhofer Institute for Material and Beam Technology IWS) for his support in laser cutting the material.

**Conflicts of Interest:** The authors declare no conflict of interest. The funders had no role in the design of the study; in the collection, analyses, or interpretation of data; in the writing of the manuscript, or in the decision to publish the results.

## References

1. Kim, S.; Laschi, C.; Trimmer, B. Soft robotics: A bioinspired evolution in robotics. *Trends Biotechnol.* **2013**, *31*, 287–294. [[CrossRef](#)] [[PubMed](#)]
2. Li, T.; Li, Y.; Zhang, T. Materials, structures, and functions for flexible and stretchable biomimetic sensors. *Acc. Chem. Res.* **2019**, *52*, 288–296. [[CrossRef](#)] [[PubMed](#)]
3. Wang, H.; Totaro, M.; Beccai, L. Toward perceptive soft robots: Progress and challenges. *Adv. Sci.* **2018**, *5*, 1800541. [[CrossRef](#)]
4. Liu, L.; Zhang, C.; Luo, M.; Chen, X.; Li, D.; Chen, H. A biologically inspired artificial muscle based on fiber-reinforced and electropneumatic dielectric elastomers. *Smart Mater. Struct.* **2017**, *26*, 85018. [[CrossRef](#)]
5. Trivedi, D.; Rahn, C.D.; Kier, W.M.; Walker, I.D. Soft robotics: Biological inspiration, state of the art, and future research. *Appl. Bionics Biomech.* **2008**, *5*, 99–117. [[CrossRef](#)]
6. Li, T.; Li, G.; Liang, Y.; Cheng, T.; Dai, J.; Yang, X.; Liu, B.; Zeng, Z.; Huang, Z.; Luo, Y.; et al. Fast-moving soft electronic fish. *Sci. Adv.* **2017**, *3*, e1602045. [[CrossRef](#)]
7. Shintake, J.; Caccuciolo, V.; Shea, H.; Floreano, D. Soft biomimetic fish robot made of dielectric elastomer actuators. *Soft Robot.* **2018**, *5*, 466–474. [[CrossRef](#)]
8. Tolley, M.T.; Shepherd, R.F.; Mosadegh, B.; Galloway, K.C.; Wehner, M.; Karpelson, M.; Wood, R.J.; Whitesides, G.M. A resilient, untethered soft robot. *Soft Robot.* **2014**, *1*, 213–223. [[CrossRef](#)]
9. Wang, W.; Ahn, S.-H. Shape memory alloy-based soft gripper with variable stiffness for compliant and effective grasping. *Soft Robot.* **2017**, *4*, 379–389. [[CrossRef](#)]
10. Kornbluh, R.D.; Pelrine, R.; Pei, Q.; Oh, S.; Joseph, J. Ultrahigh strain response of field-actuated elastomeric polymers. In *Smart Structures and Materials 2000: Electroactive Polymer Actuators and Devices (EAPAD), Proceedings of the SPIE's 7th Annual International Symposium on Smart Structures and Materials, Newport Beach, CA, USA, 6 March 2000*; Bar-Cohen, Y., Ed.; SPIE: Bellingham, WA, USA, 2000; p. 51.
11. Pei, Q.; Rosenthal, M.A.; Pelrine, R.; Stanford, S.; Kornbluh, R.D. Multifunctional electroelastomer roll actuators and their application for biomimetic walking robots. In *Smart Structures and Materials 2003: Electroactive Polymer Actuators and Devices (EAPAD), Proceedings of the Smart Structures and Materials, San Diego, CA, USA, 2 March 2003*; Bar-Cohen, Y., Ed.; SPIE: Bellingham, WA, USA, 2003; p. 281.
12. Cherif, C.; Hickmann, R.; Nocke, A.; Schäfer, M.; Röbenack, K.; Wießner, S.; Gerlach, G. Development and testing of controlled adaptive fiber-reinforced elastomer composites. *Text. Res. J.* **2018**, *88*, 345–353. [[CrossRef](#)]
13. Boyraz, P.; Runge, G.; Raatz, A. An overview of novel actuators for soft robotics. *Actuators* **2018**, *7*, 48. [[CrossRef](#)]
14. Luo, X.; Mather, P.T. Preparation and characterization of shape memory elastomeric composites. *Macromolecules* **2009**, *42*, 7251–7253. [[CrossRef](#)]

15. Kim, J.; Kim, J.W.; Kim, H.C.; Zhai, L.; Ko, H.-U.; Muthoka, R.M. Review of soft actuator materials. *Int. J. Precis. Eng. Manuf.* **2019**, *20*, 2221–2241. [[CrossRef](#)]
16. Haines, C.S.; Lima, M.D.; Li, N.; Spinks, G.M.; Foroughi, J.; Madden, J.D.W.; Kim, S.H.; Fang, S.; de Andrade, M.J.; Göktepe, F.; et al. Artificial muscles from fishing line and sewing thread. *Science* **2014**, *343*, 868–872. [[CrossRef](#)] [[PubMed](#)]
17. Cho, K.H.; Song, M.G.; Jung, H.; Park, J.; Moon, H.; Koo, J.C.; Nam, J.-D.; Choi, H.R. A robotic finger driven by twisted and coiled polymer actuator. In *Electroactive Polymer Actuators and Devices (EAPAD) 2016, Proceedings of the SPIE Smart Structures and Materials + Nondestructive Evaluation and Health Monitoring, Las Vegas, NV, USA, 20 March 2016*; Bar-Cohen, Y., Vidal, F., Eds.; SPIE: Bellingham, WA, USA, 2016; p. 97981J.
18. Motzki, P.; Gorges, T.; Kappel, M.; Schmidt, M.; Rizzello, G.; Seelecke, S. High-speed and high-efficiency shape memory alloy actuation. *Smart Mater. Struct.* **2018**, *27*, 75047. [[CrossRef](#)]
19. Anderson, I.A.; Gisby, T.A.; McKay, T.G.; O'Brien, B.M.; Calius, E.P. Multi-functional dielectric elastomer artificial muscles for soft and smart machines. *J. Appl. Phys.* **2012**, *112*, 41101. [[CrossRef](#)]
20. Madden, J.D. Mobile robots: Motor challenges and materials solutions. *Science* **2007**, *318*, 1094–1097. [[CrossRef](#)]
21. Pfeil, S.; Katzer, K.; Kanan, A.; Mersch, J.; Zimmermann, M.; Kaliske, M.; Gerlach, G. A biomimetic fish fin-like robot based on textile reinforced silicone. *Micromachines* **2020**, *11*, 298. [[CrossRef](#)]
22. Pelrine, R.; Kornbluh, R.D.; Pei, Q.; Stanford, S.; Oh, S.; Eckerle, J.; Full, R.J.; Rosenthal, M.A.; Meijer, K. Dielectric elastomer artificial muscle actuators: Toward biomimetic motion. In *Smart Structures and Materials 2002: Electroactive Polymer Actuators and Devices (EAPAD), Proceedings of the SPIE's 9th Annual International Symposium on Smart Structures and Materials, San Diego, CA, USA, 17 March 2002*; Bar-Cohen, Y., Ed.; SPIE: Bellingham, WA, USA, 2002; pp. 126–137.
23. Kellaris, N.; Gopaluni Venkata, V.; Smith, G.M.; Mitchell, S.K.; Keplinger, C. Peano-HASEL actuators: Muscle-mimetic, electrohydraulic transducers that linearly contract on activation. *Sci. Robot.* **2018**, *3*, eaar3276. [[CrossRef](#)]
24. Taghavi, M.; Helps, T.; Rossiter, J. Electro-ribbon actuators and electro-origami robots. *Sci. Robot.* **2018**, *3*, eaau9795. [[CrossRef](#)]
25. Kanik, M.; Orguc, S.; Varnavides, G.; Kim, J.; Benavides, T.; Gonzalez, D.; Akintilo, T.; Tasan, C.C.; Chandrakasan, A.P.; Fink, Y.; et al. Strain-programmable fiber-based artificial muscle. *Science* **2019**, *365*, 145–150. [[CrossRef](#)]
26. O'Brien, B.; Thode, J.; Anderson, I.; Calius, E.; Haemmerle, E.; Xie, S. Integrated extension sensor based on resistance and voltage measurement for a dielectric elastomer. In *Electroactive Polymer Actuators and Devices (EAPAD) 2007, Proceedings of the 14th International Symposium on: Smart Structures and Materials & Nondestructive Evaluation and Health Monitoring, San Diego, CA, USA, 18 March 2007*; Bar-Cohen, Y., Ed.; SPIE: Bellingham, WA, USA, 2007; p. 652415.
27. Gisby, T.A.; O'Brien, B.M.; Anderson, I.A. Self sensing feedback for dielectric elastomer actuators. *Appl. Phys. Lett.* **2013**, *102*, 193703. [[CrossRef](#)]
28. Tawfick, S.; Tang, Y. Stronger artificial muscles, with a twist. *Science* **2019**, *365*, 125–126. [[CrossRef](#)]
29. Liu, J.; Huang, J.; Su, T.; Bertoldi, K.; Clarke, D.R. Structural transition from helices to hemihelices. *PLoS ONE* **2014**, *9*, e93183. [[CrossRef](#)]
30. Godinho, M.H.; Canejo, J.P.; Feio, G.; Terentjev, E.M. Self-winding of helices in plant tendrils and cellulose liquid crystal fibers. *Soft Matter* **2010**, *6*, 5965. [[CrossRef](#)]
31. Schlatter, S.; Illenberger, P.; Rosset, S. Peta-pico-Voltron: An open-source high voltage power supply. *HardwareX* **2018**, *4*, e00039. [[CrossRef](#)]
32. Mersch, J.; Winger, H.; Nocke, A.; Cherif, C.; Gerlach, G. Experimental investigation and modeling of the dynamic resistance response of carbon particle-filled polymers. *Macromol. Mater. Eng.* **2020**, *305*, 2000361. [[CrossRef](#)]